18TH WORLD CONFERENCE ON EARTHQUAKE ENGINEERING
WCEE2024
MILAN

MILAN, ITALY
30TH JUNE - 5TH JULY 2024
www.wcee2024.it

LOCALIZATION ISSUES IN MODELLING OF SUBSTANDARD RC BEAM-COLUMN JOINTS

Y. Demirtaş[1*], Ö. Yurdakul[2] & Ö. Avşar[1]

[1] Department of Civil Engineering, Engineering Faculty, Eskişehir Technical University, Eskişehir, Türkiye, *yunus_demirtas@eskisehir.edu.tr

[2] Department of Transport Structures, Faculty of Transport Engineering, University of Pardubice, Pardubice, Czech Republic

Abstract: *Strain adjustment methods can be used in quasi-brittle materials to minimize the adverse effects of mesh size and localization in the numerical modelling of sub-standard beam-column joints. The nonlinear lattice modelling approach is adopted for this purpose. The lattice model is built using the truss analogy, in which the concrete and reinforcing elements of an RC beam-column joint are represented as truss elements. Furthermore, using zero-length springs efficiently captures the reinforcing bar slip relationship between the bars and concrete parts, which are in contact. The modelling approach is validated by comparing the simulated responses with the experimental data obtained from quasi-static cyclic loading tests conducted on two inadequately detailed sub-standard RC beam-column joints. To alleviate the issues arising from mesh size and localization, adjustments are made to the compressive strain at complete stress release in the linear softening branch, following the crack band approach. A comparison is made between the lattice model and a rigid joint model, which does not take the joint deformation into consideration. The use of the lattice modelling technique produces more realistic results by improving computing efficiency and decreasing computation time. The fidelity of the lattice modelling approach in reproducing the experimental response is deemed reasonably satisfactory.*

Keywords: Lattice modelling, Truss analogy, Crack band theory, OpenSees, Cyclic analysis.

1. Introduction

A substantial amount of the existing reinforced concrete (RC) building inventory is at risk of not achieving ductile response due to several specific local faults. These defects include the use of low-strength concrete, the presence of plain round bars, inappropriate detailing in RC components, and unaudited construction practices (Yurdakul, Duran, *et al.*, 2021). The presence of substandard beam-column joints (BCJs) in a moment-resisting reinforced concrete (RC) building frame contradicts the capacity design concepts employed in the design of earthquake-resistant structural systems. These BCJs, being one of the weakest and most vulnerable components adversely affects the resilience of the structure. The presence of structurally deficient RC components causes an unacceptably high risk of severe damage, particularly in vulnerable RC structures, at which the initiation of a global failure mechanism is highly probable. Moreover, assessing the predicted behavior and severity of damage in BCJs is gaining significance for substandard RC buildings. Nonlinear numerical models have the capability to do this task. Nevertheless, the reliability of models and the accuracy

of structural response predictions is questionable for substandard RC BCJs. The rigid joint assumption in structural analysis fails to accurately capture the actual deformations in vulnerable RC BCJs, whose response is predominantly controlled by the inherent nonlinear deformations. The strategy of assuming rigid joints, although easy and simple for defining subassemblies, is inadequate in accurately representing the behaviour of such BCJs (Adom-Asamoah and Osei, 2018). The spring modelling methodology is widely recognized as a practical, time-efficient c and computationally stable approach when the effects of joint deformability is properly considered (Alath and Kunnath, 1995; Lowes and Altoontash, 2003). Moreover, the current spring models have been improved, and new models with higher predictive capabilities have been developed (Celik and Ellingwood, 2008; Hassan and Moehle, 2012; Girgin, Polat and Misir, 2021). Moreover, the utilization of 2D or 3D continuum elements of the finite element method (FEM) in computer-aided nonlinear analysis software may yield the most accurate approximations of the actual response (Santarsiero, 2018; Yurdakul, Del Vecchio, et al., 2020; Yurdakul, Tunaboyu, et al., 2020). Nevertheless, the extensive computing time and effort hinder the widespread adoption of FEM in structural analysis.

The effectiveness of the lattice modelling approach is ascertained by a precise reproduction of the behavior shown by different RC components (Niwa, Choi and Tanabe, 1995; Park and Eom, 2007; Lu and Panagiotou, 2014; Alvarez et al., 2019; Deng et al., 2021; Aydin et al., 2022). Bowers, (2014) proposed a lattice model for the behavior of three nonductile RC BCJs, consisting of one exterior joint and two interior joints. The currently available lattice models have demonstrated a high level of accuracy in predicting the failure of shear-dominated BCJs when subjected to quasi-static cyclic stresses. Moreover, the lattice model effectively predicts the yielding of beam longitudinal reinforcement, together with the occurrence of diagonal compression. Xing et al., (2018) employed FEM and lattice modelling techniques to predict the response of RC joints. Truss models provide the capability to predict the damage patterns of BCJ structures and the overall hysteretic response. Xing, (2019) employed finite element (FE) and lattice modelling techniques to examine the behavior of flexural-shear-bond interaction of two-way beam-column-slab internal joints. The results of the experiment were compared with the local performance of the reinforcing bar, including in terms of bond-slip and strain history. The accuracy and efficacy of FE approach were compared to those of the lattice modelling for an equal set of joints. The lattice modelling technique demonstrated higher accuracy compared to alternative methodologies in relation to several aspects of global and local responses. These include the analysis of the hysteretic curve, the development of local bond-slip behavior, and the distribution of stress and strain along the longitudinal bars of the beam. The lattice model has the potential to provide a reasonable overall response, particularly in cases where it successfully captures significant shear cracks. Girgin, (2020) examined the effects of BCJ modelling on the evaluation of performance in nonductile RC frames. Two BCJs were developed using the lattice modelling approach, employing two different mesh sizes. The lattice modelling approach for BCJs effectively reproduces the reported joint behavior.

Although the lattice modelling technique has been used in earlier research for various RC components, the strain adjustment for quasi-brittle materials (i.e., concrete) to reduce the mesh size impact and localization concerns in the lattice modelling of BCJs has received less attention. The novelty of this work lies in the strain adjustment for substandard RC BCJs using a nonlinear lattice modelling technique. The truss analogy is used to construct lattice models with varied mesh sizes of poorly detailed two substandard RC BCJs tested under quasi-static cyclic loads. The strain-based softening function in the uniaxial material property of concrete is adjusted using the crack band technique (Bažant and Oh, 1983) to reduce the mesh size effect and localization difficulties. The simulated reactions are validated in comparison to the experimental results.

2. Lattice modelling of beam-column joints

A nonlinear lattice structure is generated for the studied test specimens by employing the horizontal, vertical, and diagonal truss components to simulate the behavior of BCJs in OpenSees, (McKenna et al., 2016). The reinforcement bar-slip relationship is captured by including nonlinear springs with zero-length elements that are connected to both the reinforcing steel and concrete elements. The schematic representation of the lattice model for a BCJ is illustrated in Figure 1. The utilization of the nonlinear force-based beam-column element is employed to model the beam and column elements in areas where the damage is not localized, with the aim of minimizing computing demands. The fiber section model represents these components. The elastic section properties of the rigid interface elements of the BCJ are relatively larger, since they link the beam and column elements with the lattice elements.

Figure 2 (a and b) show the cross-sectional areas of the concrete truss members. The product of the out-of-plane thickness *w* and half of the tributary width yields the cross-sectional areas of the vertical and horizontal concrete truss members. The effective width of the diagonal concrete members, on the other hand, is determined using Eq. (1), which was presented by Xing (2019). The diagonal members' cross-sectional areas are determined as the product of the out-of-plane thickness w and half of the effective width beff. The overlapping of the tributary widths of the concrete truss members is the rationale for utilizing half-width for all concrete truss members (Demirtas, 2022).

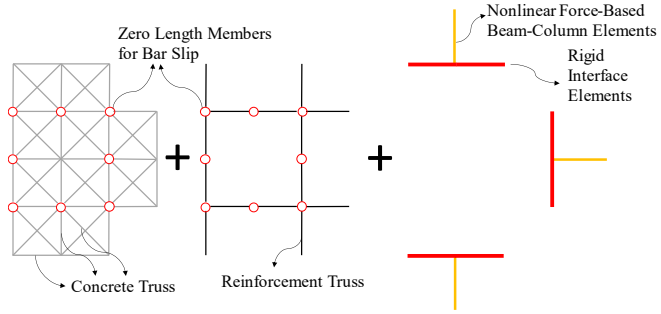

Figure 1. Layout of the lattice model for BCJ

(a) *(b)*

Figure 2. Details of the concrete truss members (a) tributary widths of the horizontal and vertical concrete truss members (b) tributary width of the diagonal concrete truss members

$$b_{eff} = \frac{a\ x\ b}{\sqrt{a^2 + b^2}} \quad (1)$$

where, *a* and *b* are the horizontal and vertical width of the mesh element, respectively.

The quantity of reinforcing steel in the test specimen is used to compute the cross-sectional areas of the reinforcement truss members. A single equivalent reinforcement is defined at the same elevation. For consistency, reinforcement truss members are positioned at the borders of the RC sections to locate the reinforcement at the same locations in all lattice models with varying mesh sizes. To model the interaction between the joint and the neighbouring beam or column element, a rigid beam-column element is employed. To maintain structural integrity, EqualDof constraints in the x and y directions for the translational degree of freedom are assigned at the connection nodes at the truss members and the rigid interface elements.

2.1. Concrete model

The ConcretewBeta Material model, developed by Lu and Panagiotou, (2014) defines concrete's tensile and compressive behavior. Concrete stress-strain defined by this material model, which is already available in OpenSees, is shown in Figure 3 (a). The variable f_c in the current model represents concrete's maximum compressive strength at ε_0 strain. The symbol ε_u represents the maximum strain of unconfined concrete. The coefficient α, which controls unloading under tensile strain, is typically set to 1 by default. The model parameters are based on concrete compressive strength, which is determined by sample tests for each case study. It is assumed that the strain at the maximum compressive strength ε_0 is consistent (0.002) in all specimens containing low-strength concrete. In contrast, mesh size was accounted for by modifying strain based on truss element length. This adjustment was made to the linear softening branch of the model (Figure

3 (a and b)). Lack of objectivity in the softening regime of concrete models is a major drawback. If localization is ignored, Binici (2005) suggests that softening zone response may be inconsistent regardless of the function employed for the material model. Coleman and Spacone, (2001) proposed a regularization method for force-based beam-column elements' compressive stress-strain characteristics. This strategy aims to release energy uniformly after strain-softening. The Kent-Park concrete model (Kent and Park, 1971) used the method, as shown in Figure 3 (b). The shaded region in this model represents the energy released during strain softening, denoted as G_f^c (N/m). Each assumption is based on the crack band technique proposed by Bažant and Oh (1983). The strain at complete stress release ε_u is the ratio of plastic displacement w_d to the truss element size L_t, as shown in Eq. (2) (Bažant and Oh, 1983). The strain at complete stress release, ε_u, is calibrated to the mesh size to maintain a constant energy value G_f^c. For specimens with a height of 300 mm, Duran et al., (2017) found that the plastic displacement w_d, which is the point at which low-strength concrete (8-12 MPa) strength drops to zero, was around 7 mm on average. Given the test specimens' similar concrete strength to Duran et al. (2017), corresponding strains are modified.

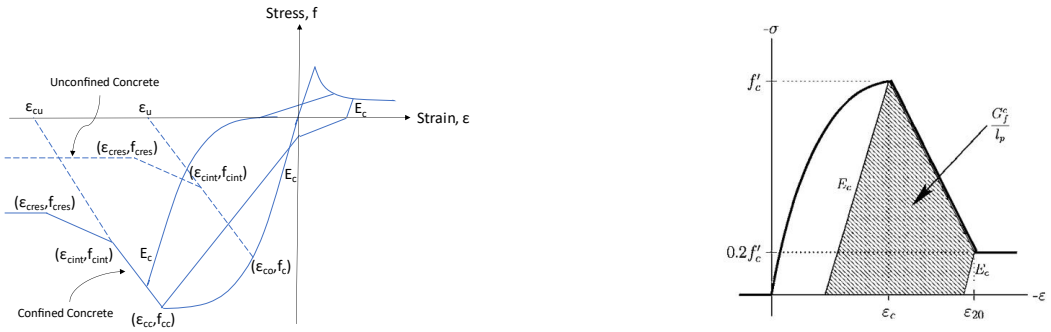

(a) *(b)*

Figure 3. (a) Uniaxial stress strain relationship of concrete (Lu and Panagiotou, 2014) (b) Kent–Park concrete stress–strain model with fracture energy G_f^c in compression as shaded area (Scott and Fenves, 2006)

The defined tensile behavior takes into account the softening regime. Nevertheless, in order to ensure computational stability, the ultimate tensile strain ε_t, at which the tensile stress becomes zero (as seen in Figure 3 (a)), is established as 1.0 to prevent the occurrence of tensile failure in concrete.

$$\varepsilon_u = w_d / L_t \tag{2}$$

where, ε_u is the ultimate strain, w_d is the plastic displacement and L_t is the length of the concrete truss member.

Cracked concrete must reduce compressive strength. Vecchio and Collins, (1986) recommend considering transverse strain when analyzing diagonal concrete components. The compressive strength f_c of concrete decreases as the transverse strain ε_n increases in the tensile direction. This reduction is achieved by using the multiplier β. Following Kollegger and Mehlhorn, (1988), adapting a residual value β_{res} of 0.45,the numerical instability is observed in the specimen with low-strength concrete (8-10 MPa). Therefore, the β_{res} value recommend by Kollegger and Mehlhorn, (1988) is used for the specimen with normal strength concrete. Dyngeland's (1989) recommendation (i.e., β_{res} value of 0.8) is used for the specimen with low strength concrete. A Gaussian relationship between strength decrease β and transverse strain ε_n is often depicted, as stated by Červenka, Jendele and Červenka, (2013). Figure 4 shows how a tri-linear connection can represent the smooth Gaussian form. Thus, the chosen β_{int} values at the end are 0.9 (for β_{res}= 0.8) and 0.6 (for β_{res}= 0.45).

In order to monitor transverse strain for a single element, it is necessary to build four nodes. Figure 4 illustrates that out of the four nodes, two nodes are responsible for defining a concrete truss element, while the other two nodes form a gauge element with zero-stiffness. Typically, the two transverse nodes are regarded as the remaining nodes of the cell due to their inclusion as diagonal components. Therefore, the establishment of a meshing pattern that closely resembles a square shape is advantageous for concrete. The computation of

transverse strain include the consideration of the element's length. The values of ε_{int} and ε_{res} decrease proportionally with the increase in the length of the concrete truss member. The values of ε_{int} and ε_{res} are determined using Eqs. (3) and (4) respectively, as originally proposed by Lu and Panagiotou, (2014).

In general, because the diagonal components are part of a cell, two transverse nodes are considered as the cell's remaining two nodes. As a result, creating a close-to-square meshing for concrete is favorable. The element length is taken into account in the calculation of transverse strain. The corresponding values of ε_{int} and ε_{res} reduce as the length of the concrete strut member increases. ε_{int} and ε_{res} are calculated from Eqs, (3) and (4) respectively which were proposed by Lu and Panagiotou, (2014).

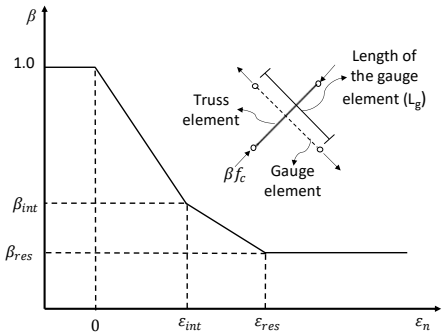

Figure 4. Strength reduction factor with transverse strain (McKenna et al., 2016)

$$\varepsilon_{int} = \left(600/L_g\right) x\ 0.01 \tag{3}$$

$$\varepsilon_{res} = \left(600/L_g\right) x\ 0.025 \tag{4}$$

where L_g is the total length of gauge elements in mm as shown in Figure 4.

2.2. Reinforcement model

The present analysis incorporates the ReinforcingSteel material model from OpenSees, which is derived from the uniaxial steel model proposed by Chang and Mander, (1994). If accessible, the values of yielding and ultimate strain are obtained from the material tests done on the test specimen under consideration. Alternatively, the material properties recommended by the Turkish Building Earthquake Code (TBEC, 2018) are employed. The link between reinforcement bar-slip is represented by the utilization of zero-length springs that are connected to both the reinforcing steel and concrete elements, employing the uniaxial material model. Even though computational friendly models are available (Yurdakul, Balaban, et al., 2021; Yurdakul et al., 2022). The parameters of the BarSlip model are determined by the evaluation of the Pinching4 material model in OpenSees, as seen in Figure 5. The terms S_{lim}^{C} and S_{lim}^{T} denote the slip limit in compression and tension, correspondingly. Additionally, the terms F_{lim}^{C} and F_{lim}^{T} denote the force limits in compression and tension, respectively. The development of the bond-slip relationship's backbone curve involves the consideration of several factors, including the compressive strength of the concrete, the yield and ultimate strength of the reinforcing steel, the elasticity modulus of the reinforcing steel, as well as the diameter and number of the reinforcing bars.

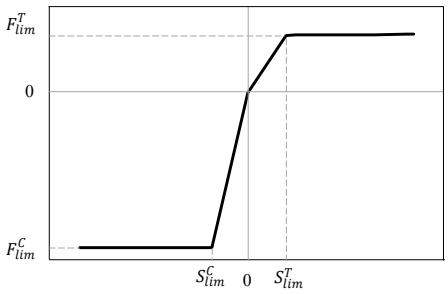

Figure 5. Backbone curve of the BarSlip material model (Pinching4) (Demirtas, Yurdakul and Avşar, 2023)

3. Case studies

This study focuses on the investigation of two substandard BCJ specimens that were exposed to reversed cyclic quasi-static stress using the lattice modelling technique. The selection of test specimens takes into account both the inadequate configuration arising from typical flaws in existing RC structures and their failure mechanisms. Subsequently, a comparison is made between the results obtained from the lattice models and the experimental findings. Table 1 provides comprehensive information on the unique characteristics and primary attributes of the specimens. The initial joint specimen employed in the present investigation is referred to as EJ-R (Yurdakul and Avşar, 2016), while the subsequent joint specimen is denoted as O_2 (Tsonos, 2008).

Table 1. Main properties of the test specimens

Property	**Test Specimens**	
	EJ-R (Yurdakul and Avşar, 2016)	**O_2 (Tsonos, 2008)**
Concrete Compressive Strength, f_c (MPa)	8.05	16.2
Reinforcement Yield Strength, f_y (MPa)	292.5	540
Type of longitudinal reinforcement	Plain	Deformed
Beam cross-section	250 x 500 mm	200 x 300 mm
Column cross-section	250 x 500 mm	200 x 200 mm
Column axial load ratio, N_d/f_cA_c	0.1	0.25
Failure mode	Joint shear	Joint shear
Spacing of transverse reinforcement in column (mm)	Ø10/150	Ø6/150
Spacing of transverse reinforcement in beam (mm)	Ø10/100	Ø8/70
Longitudinal reinforcement ratio of the column (%)	1.63	1.54
Longitudinal reinforcement ratio of the beam (%)	2.08	2.01

3.1. Specimen 1: EJ-R

The test specimen used in the study conducted by Yurdakul and Avşar (2016), referred to as EJ-R, is representative of the predominant external beam-column joint (BCJ) subassembly seen in substandard reinforced concrete (RC) structures in Türkiye and the Mediterranean region. The specimen is found to be in violation of many design principles outlined in both contemporary and past seismic design standards. The BCJ has a deficiency in transverse reinforcement, as seen in Figure 6 (a). In order to reduce the shear capacity of the BCJ, a value of $0.1A_cf_c$ is chosen for the column. This value corresponds to the minimum axial load required for columns as defined in the Turkish Earthquake Code 2007 (TEC-2007, 2007). The specimens are subjected to quasi-static cyclic loading while simultaneously applying a constant axial stress. Additional comprehensive details on the specimen may be found in the publication by Yurdakul and Avşar (2016).

In order to assess the reliability of the strain adjustment, several mesh sizes, specifically 0.25 m, 0.125 m, 0.1 m, and 0.05 m, are used in the creation of the lattice model of EJ-R in the OpenSees software. The schematic representation of the lattice model with a mesh size of 0.25 m is seen in Figure 6 (b).

Figure 7 presents a comparison between the numerical outcomes and the experimental results in relation to the hysteric response, considering various mesh sizes of the lattice model for EJ-R. It is important to observe that the convergence of all numerical models occurred due to the minimization of strain localization effects through the implementation of strain adjustment techniques. The model's accuracy, with respect to overall behavior, exhibits close comparability across all mesh sizes. The model with a mesh size of 0.25 m exhibited an overestimation of peak strength when compared to the other models employing a finer mesh. Furthermore, the accuracy of predicting the post-peak behavior is similarly decreased. Despite the potential reduction or elimination of mesh sensitivity by strain adjustment, the iterative process of the nonlinear numerical solution remains susceptible to variations in mesh size. The observed variation in the models with varying mesh sizes is attributed to numerical instabilities encountered during the iterative solution process. Therefore, the model

that utilizes a mesh size of 0.125 m demonstrates improved accuracy in replicating the peak and post-peak response. The model with a mesh size of 0.1 m demonstrates an even higher level of effectiveness in predicting the same response numbers. The lattice model with a mesh size of 0.05 m exhibits comparable peak strength and post-peak response to the model with a mesh size of 0.1 m, while outperforming other models in terms of producing results that closely align with experimental findings.

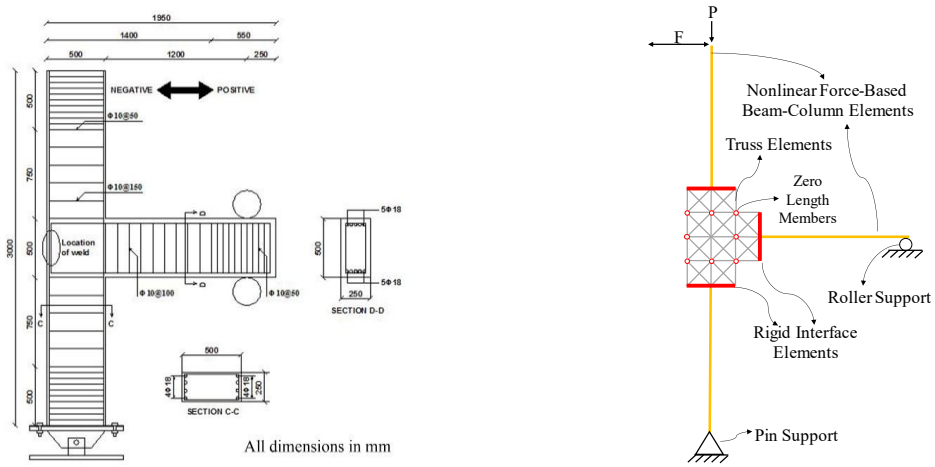

(a) *(b)*

Figure 6. Details of the specimen EJ-R (a) dimensions and reinforcement details of the specimen EJ-R (b) general layout of the EJ-R model

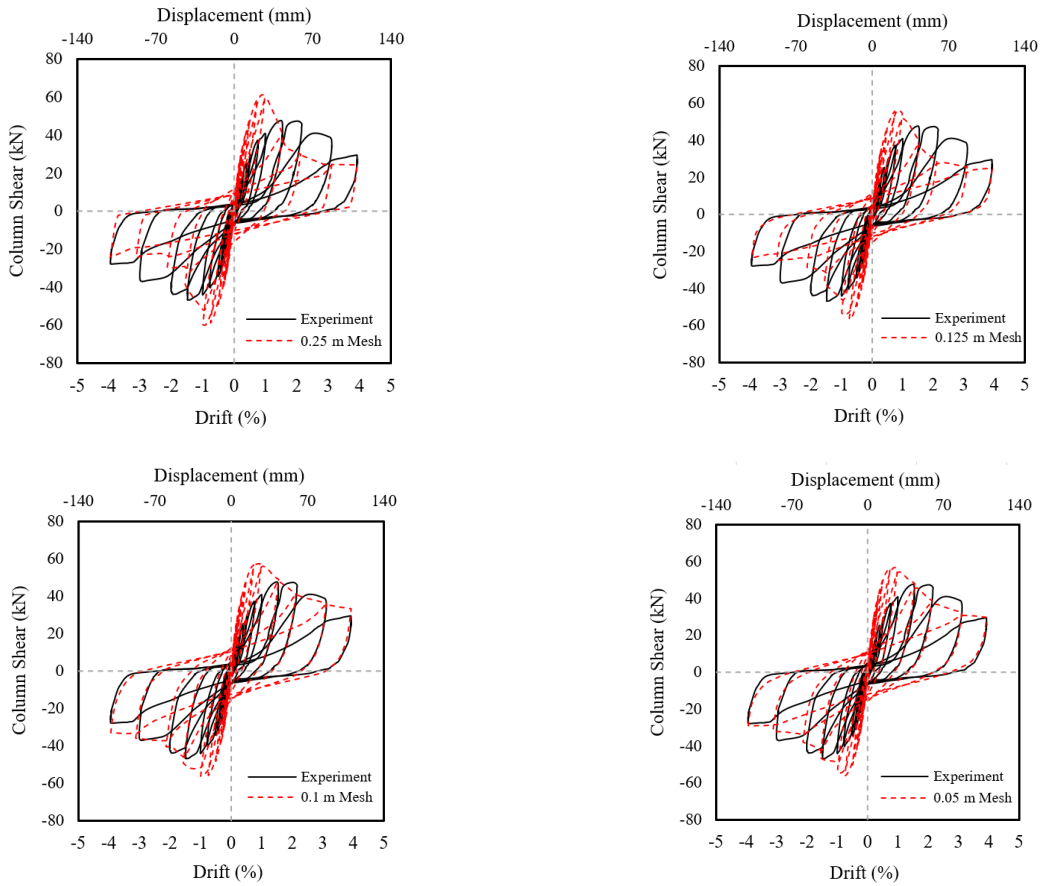

Figure 7. Comparison of hysteresis curves of EJ-R for the experimental and lattice models with different mesh sizes

After verifying the model's accuracy, a numerical examination evaluates the assumption of rigid joint behavior, specifically ignoring joint deformations. The rigid joint model connects beams and columns at a node, imposing a single rotational degree of freedom at structural member ends. The analysis results are systematically compared to lattice models with different mesh sizes, as shown in Figure 8. The rigid model predicts significantly different results from experiment. The flexural response or yielding of the reinforcing steel bars in the beam, controls the behavior of the model with nondeformable joints. This does not accurately reflect the overserved experimental response, emphasizing the need to consider joint deformations when assessing substandard RC structures.

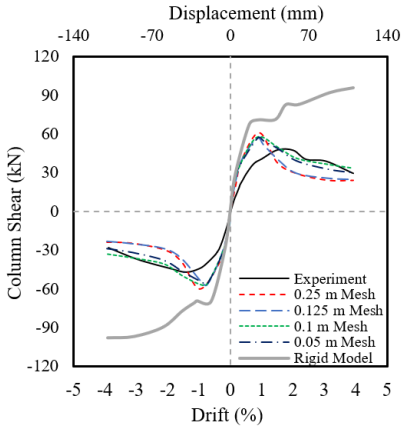

Figure 8. Comparison of envelope curves of EJ-R for the experimental, lattice model with different mesh sizes and rigid joint model

3.2. Specimen 2: O_2

The second test specimen evaluated in this study is the external BCJ, referred to as O_2 by Tsonos (2008). The specimen was manufactured using design and detailing procedures that did not adhere to established standards. As seen in Figure 9 (a), the dimensions of the specimen's column are 200 x 200 x 1400 mm. The cross-sectional dimensions of the beam in the plane are 200 x 300 mm, and its length is 950 mm. The structure under consideration is a beam with an out-of-plane configuration. The beam has a rectangular cross-section of 100 x 200 mm and a length of 200 mm. It is connected at a junction. The RC slab, which is positioned above the beams, has a uniform thickness of 50 mm. Notably, it extends by a length of 200 mm on a single side of the beam only. The experimental setup involves subjecting the beam's end to a quasi-static cyclic displacement, with one complete cycle for each loading level. This displacement is applied while the column is subjected to a constant axial load, with an axial load ratio of $0.25A_cf_c$.

The lattice model of the specimen O_2 is developed in OpenSees. Three square mesh sizes, namely 0.1 m, 0.05 m, and 0.025 m, are utilized in the simulations. The schematic representation of the model is presented in Figure 9 (b). Similar to the previously examined EJ-R specimen, the column and beam components are simulated using a nonlinear force-based beam-column element. The lower end of the column is pinned, while the upper end of the column is restricted to movement only along the axis of the column. The lateral cycle load is applied at the end of the beam in vertical direction.

The comparative study of the reversed cyclic results of the O_2 specimen, which is simulated using a lattice model with varying mesh sizes, is presented in Figure 10 with the corresponding experimental findings. The response metrics, including initial stiffness and peak response, exhibit satisfactory agreement with the experimental findings, independent of the mesh size utilized. As the mesh structure changes from a coarse resolution of 0.1 m to a finer resolution of 0.05 m, numerically obtained post-peak response of the specimen becomes closed to the experimental result. The prediction accuracy of the numerical model for the finest mesh structure with a spacing of 0.025 m is similar to that of previous models in terms of initial stiffness and peak strength. However, the model with the finest mesh structure was unable to precisely represent the post-peak response, particularly in the negative direction. The damage is mostly localized at the joint back, leading to significant tensile stresses and slip demands in the bottom reinforcing steel, as well as the truss member. Hence, the numerical anaysis was unable to proceed for the entire displacement history and terminated at 3%

drift ratio, the strain adjustment applied to the numerical model with the finest mesh was unable to address the problem of localization effectively, leading to numerical instability in successive stages of drift.

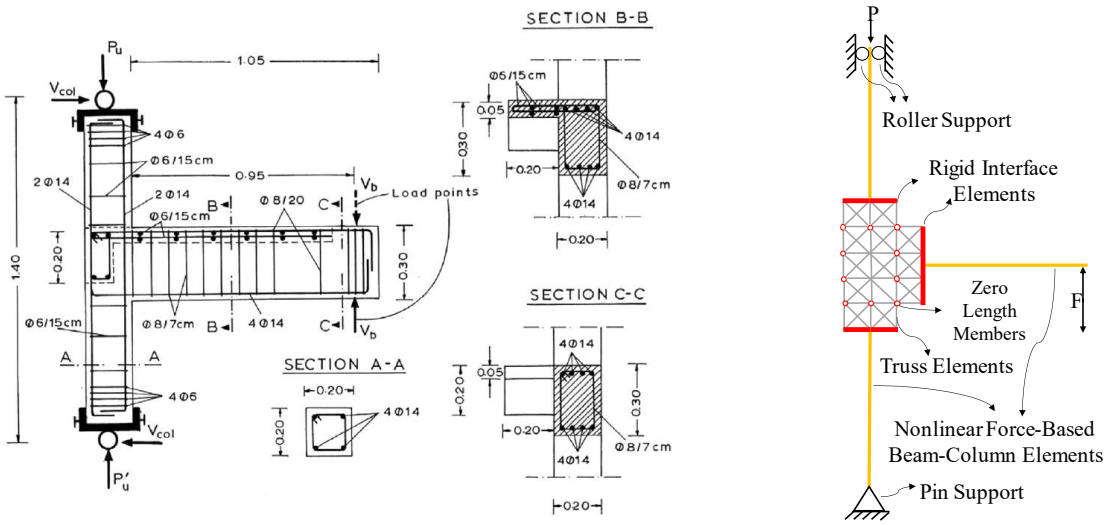

Figure 9. Details of the specimen O_2 (a) dimensions and reinforcement details of the specimen O_2 (b) general layout of the lattice model for O_2

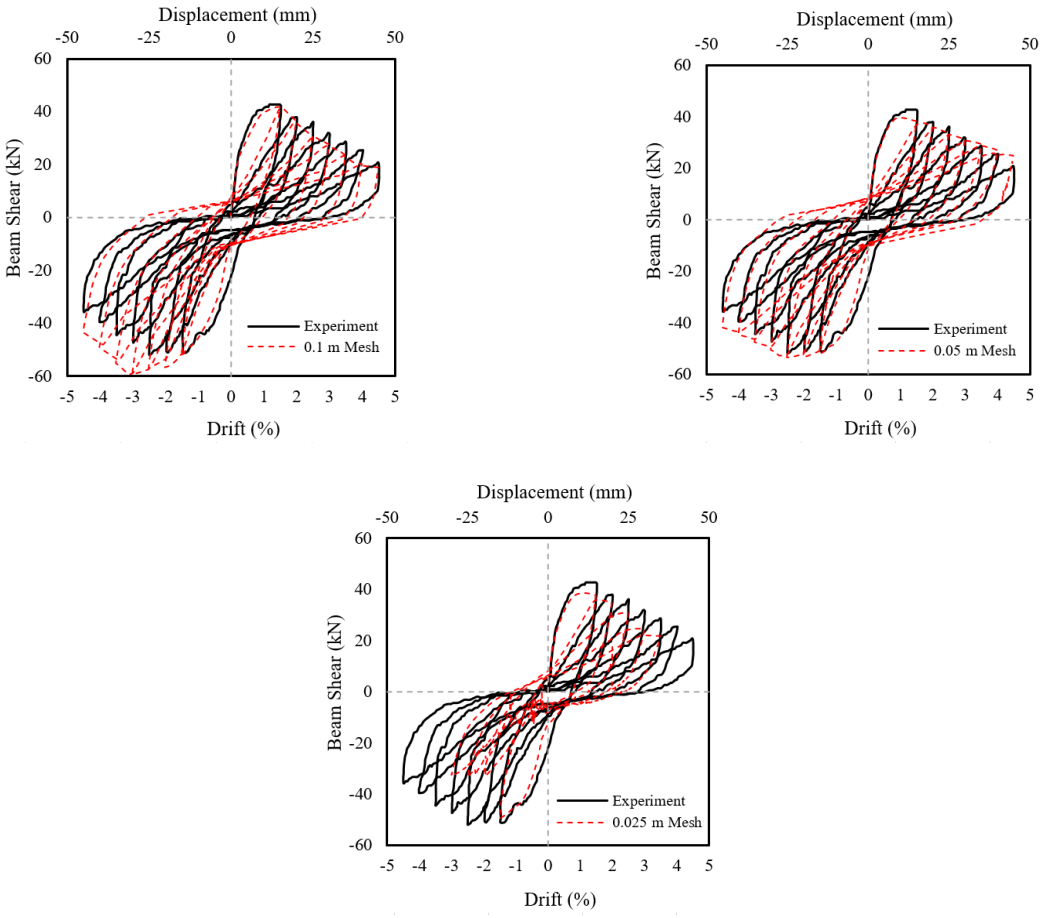

Figure 10. Comparison of hysteresis curves of O_2 for the experimental and lattice models with different mesh sizes

In order to examine the difference between the responses of rigid and deformable joints, the outcomes of the lattice models with varying mesh sizes are compared with those of the rigid model, which ignores deformations in the joint region (Figure 11). As predicted, the rigid joint model was unable to accurately predict the decline in strength of the specimen due to the imposed damage in the joint (BCJ). The overall behavior of the rigid joint model is mostly influenced by the flexural response of the subassembly.

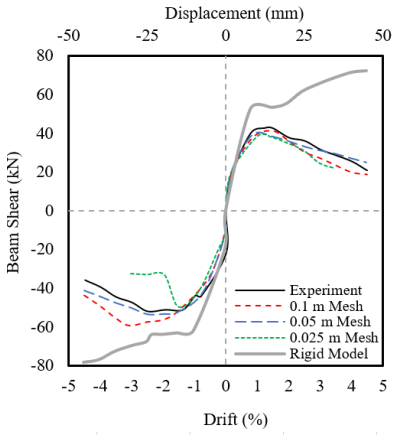

Figure 11. Comparison of envelope curves of O_2 for the experimental, lattice model with different mesh sizes and rigid joint model

4. Conclusion

This study investigates strain adjustment for quasi-brittle materials to reduce mesh size effect and localization issues. The investigation uses nonlinear lattice modelling for substandard BCJs. The lattice modelling method represents RC BCJ concrete and reinforcement members as truss elements with different material properties. Diagonal concrete members consider transverse tensile strain on compressive strength. Zero-length springs connected to steel and concrete elements simulate reinforcement bar slip. The strain-based softening function of concrete is modified according to crack band theory to reduce mesh size and localization issues. The modelling technique is validated by comparing the simulated and experimental responses of two insufficiently detailed RC BCJs (EJ-R and O_2). Mesh sensitivity in lattice models requires several mesh sizes for each test specimen based on geometry and cross-section details.

Based on the results of cyclic analyses using the lattice modelling method for the two tested specimens, following conclusions can be drawn:

- The application of a lattice structure including truss elements demonstrates a good performance to accurately predict the response variables of shear critical substandard RC BCJs when exposed to cyclic loads. The mesh sensitivity of lattice models for RC BCJs can be reduced by strain adjustment, since the models with varying mesh sizes provide similar numerical results.
- The analytical results of the numerical models using rigid joint assumptions exhibit a lack of compatibility with the experimental data. The dominant behavior of the model with nondeformable joints is determined by the flexural response of the beam, namely the yielding of the reinforcing steel bars of the beam. The rigid joint assumption adopted for the shear critical BCJ test specimens does not accurately represent the actual response. This highlights the significance of taking joint deformations into account in substandard RC constructions.
- The lattice modelling technique is able to effectively represent the global hysteretic response, while requiring less computing work for all the specimens that were studied. This is due to its conceptual simplicity and efficiency.

5. References

Adom-Asamoah, M. and Osei, J. B. (2018) ‘A comparative seismic fragility analysis of a multi and single component beam-column joint models’, *Cogent Engineering*. Cogent, 5(1426204), pp. 1–18. doi: 10.1080/23311916.2018.1426204.

Alath, S. and Kunnath, S. K. (1995) 'Modeling Inelastic Shear Deformation in RC Beam-Column Joints', in *Proceedings of the 10th Conference on Engineering Mechanics. Part 2 (of 2)*. Boulder, CO, USA: ASCE, New York, NY, USA, pp. 822–825.

Alvarez, R. *et al.* (2019) 'Nonlinear cyclic Truss Model for analysis of reinforced concrete coupled structural walls', *Bulletin of Earthquake Engineering*. Springer Netherlands, 17, pp. 6419–6436. doi: 10.1007/s10518-019-00639-8.

Aydin, B. B. *et al.* (2022) 'Lattice modeling and testing of aerated autoclaved concrete infilled frames', *Engineering Structures*. Elsevier Ltd, 251, p. 113467. doi: 10.1016/j.engstruct.2021.113467.

Bažant, Z. P. and Oh, B. H. (1983) 'Crack band theory for fracture of concrete', *Matériaux et Construction*, 16(3), pp. 155–177. doi: 10.1007/BF02486267.

Binici, B. (2005) 'An analytical model for stress-strain behavior of confined concrete', *Engineering Structures*, 27, pp. 1040–1051. doi: 10.1016/j.engstruct.2005.03.002.

Bowers, J. T. (2014) *Nonlinear Cyclic Truss Model for Beam-Column Joints of Non-ductile RC Frame*. Virginia Polytechnic and State University.

Celik, O. C. and Ellingwood, B. R. (2008) 'Modeling beam-column joints in fragility assessment of gravity load designed reinforced concrete frames', *Journal of Earthquake Engineering*, 12, pp. 357–381. doi: 10.1080/13632460701457215.

Červenka, V., Jendele, L. and Červenka, J. (2013) 'ATENA Program Documentation Part 1 Theory', p. 268.

Chang, G. A. and Mander, J. B. (1994) *Seismic Energy Based Fatigue Damage Analysis of bridge Columns: Part 1 - Evaluation of Seismic Capacity*.

Coleman, J. and Spacone, E. (2001) 'Localization Issues in Force-Based Frame Elements', *Journal of Structural Engineering-asce - J STRUCT ENG-ASCE*, 127. doi: 10.1061/(ASCE)0733-9445(2001)127:11(1257).

Demirtas, Y. (2022) *Lattice Modelling of Sub-Standard Reinforced Concrete Beam-Column Joints*. Eskişehir Technical University.

Demirtas, Y., Yurdakul, Ö. and Avşar, Ö. (2023) 'Lattice modelling of substandard RC beam-column joints considering localization issues', 47(January), pp. 2515–2530. doi: 10.1016/j.istruc.2022.12.062.

Deng, X. *et al.* (2021) 'Nonlinear truss models for strain-based seismic evaluation of planar RC walls', *Earthquake Engineering and Structural Dynamics*, 50, pp. 2939–2960. doi: 10.1002/eqe.3480.

Duran, B., Tunaboyu, O. and Avşar, Ö. (2017) 'Düşük dayanimli betonun elastisite modülünün belirlenmesi ve RYTEİE ile yapilan risk değerlendirmesine etkisi', *Journal of the Faculty of Engineering and Architecture of Gazi University*, 32(1), pp. 275–286. doi: 10.17341/gazimmfd.300617.

Dyngeland, T. (1989) *Behavior of Reinforced Concrete Panels, Dissertation, BK-report 1989:1*. Norway.

Girgin, S. C. (2020) 'Effect of modeling beam-column joints on performance assessment of columns in non-ductile RC frames', *Teknik Dergi/Technical Journal of Turkish Chamber of Civil Engineers*, 31(6), pp. 10339–10358. doi: 10.18400/TEKDERG.456752.

Girgin, S., Polat, F. and Misir, I. (2021) 'Mevcut Betonarme Binalarda Kolon-Kiriş Birleşimi Modellemesinin Etkileri', in *6. Uluslararası Deprem Mühendisliği ve Sismoloji Konferansı*. Gebze, Kocaeli.

Hassan, W. M. and Moehle, J. P. (2012) 'Experimental Assessment of Seismic Vulnerability of Corner Beam-Column Joints in Older Concrete Buildings', *15th World Conference on Earthquake Engineering (15WCEE)*.

Kent, D. C. and Park, R. (1971) 'Flexural Members with Confined Concrete', *Journal of the Structural Division*, 97(7), pp. 1969–1990.

Kollegger, J. and Mehlhorn, G. (1988) 'Experimentelle und Analytische Untersuchungen zur Aufstellung eines Materialmodels für Gerissene Stahbetonscheiben', *Nr.6 Forschungsbericht, Massivbau, Gesamthochschule Kassel*.

Lowes, L. N. and Altoontash, A. (2003) 'Modeling Reinforced-Concrete Beam-Column Joints Subjected to Cyclic Loading', *Journal of Structural Engineering*. American Society of Civil Engineers (ASCE), 129(12), pp. 1686–1697. doi: 10.1061/(asce)0733-9445(2003)129:12(1686).

Lu, Y. and Panagiotou, M. (2014) 'Three-Dimensional Cyclic Beam-Truss Model for Nonplanar Reinforced Concrete Walls', *Journal of Structural Engineering*, 140(3), p. 04013071. doi: 10.1061/(asce)st.1943-541x.0000852.

McKenna, F. *et al.* (2016) 'OpenSees: Open system for earthquake engineering simulation. http://opensees.berkeley.edu'.

Niwa, J., Choi, I.-C. and Tanabe, T. (1995) 'Analytıcal Study For Shear Resıstıng Mechanısm Usıng Lattıce Model', *Concrete Library of JSCE*, 26, pp. 95–109.

Park, H. and Eom, T. (2007) 'Truss Model for Nonlinear Analysis of RC Members Subject to Cyclic Loading', *Journal of Structural Engineering*, 133(10), pp. 1351–1363. doi: 10.1061/(asce)0733-9445(2007)133:10(1351).

Santarsiero, G. (2018) 'FE modelling of the seismic behavior of wide beam-column joints strengthened with CFRP systems', *Buildings*, 8(31). doi: 10.3390/buildings8020031.

Scott, M. H. and Fenves, G. L. (2006) 'Plastic Hinge Integration Methods for Force-Based Beam–Column Elements', *Journal of Structural Engineering*, 132(2), pp. 244–252. doi: 10.1061/(asce)0733-9445(2006)132:2(244).

TBEC (2018) 'Turkish Building Earthquake Code', *Disaster and Emergency Management Presidency*, p. 416. Available at: http://www.resmigazete.gov.tr/eskiler/2018/03/20180318M1.pdf.

TEC-2007 (2007) *Turkish Earthquake Code, Ministry of Public Works and Settlement*. Ankara.

Tsonos, A. G. (2008) 'Effectiveness of CFRP-jackets and RC-jackets in post-earthquake and pre-earthquake retrofitting of beam-column subassemblages', *Engineering Structures*, 30(3), pp. 777–793. doi: 10.1016/j.engstruct.2007.05.008.

Vecchio, F. J. and Collins, M. P. (1986) 'The Modified Compression-Field Theory for Reinforced Concrete Elements Subjected To Shear', *ACI Journal*, 83(22), pp. 219–231.

Xing, C. *et al.* (2018) 'Computational simulation of RC beam-to-column connections under earthquake loading', in *11th National Conference on Earthquake Engineering 2018, NCEE 2018: Integrating Science, Engineering, and Policy*. Los Angeles, CA.

Xing, C. (2019) *An Analytical Study on the Behavior of Reinforced Concrete Interior Beam-Column Joints*. Virginia Polytechnic Institute and State University.

Yurdakul, Ö., Del Vecchio, C., *et al.* (2020) 'Numerical simulation of substandard beam-column joints with different failure mechanisms', *Structural Concrete*, 21, pp. 2515–2532. doi: 10.1002/suco.201900003.

Yurdakul, Ö., Tunaboyu, O., *et al.* (2020) 'Parameter sensitivity of CFRP retrofitted substandard joints by stochastic computational mechanics', *Composite Structures*, 238, p. 112003. doi: https://doi.org/10.1016/j.compstruct.2020.112003.

Yurdakul, Ö., Duran, B., *et al.* (2021) 'Field reconnaissance on seismic performance of RC buildings after the January 24, 2020 Elazığ-Sivrice earthquake', *Natural Hazards*. Springer Netherlands, 105(1), pp. 859–887. doi: 10.1007/s11069-020-04340-x.

Yurdakul, Ö., Balaban, E., *et al.* (2021) 'Stochastic assessment of bond-slip behavior of plain round bars in low strength concrete', *Engineering Structures*, 229(April 2020). doi: 10.1016/j.engstruct.2020.111658.

Yurdakul, Ö. *et al.* (2022) 'Evaluation of cyclic bond-slip behavior of smooth bars in low strength concrete: An experimental and stochastic study', *Structures*. Elsevier, 41, pp. 568–585. doi: 10.1016/J.ISTRUC.2022.05.036.

Yurdakul, Ö. and Avşar, Ö. (2016) 'Strengthening of substandard reinforced concrete beam-column joints by external post-tension rods', *Engineering Structures*, 107, pp. 9–22. doi: 10.1016/j.engstruct.2015.11.004.